

Segmentation of a road from a vehicle-mounted radar and accuracy of the estimation

Mila Nikolova

Dept. TSI
ENST
Paris, 75013
nikolova@tsi.enst.fr

Alfred Hero III

Dept. EECS
University of Michigan
Ann Arbor MI 48109-2122
hero@eecs.umich.edu

Abstract

This work treats a problem relevant to automatic road following, collision avoidance, and maneuver control. A millimeter-wave radar is placed on the front of the vehicle and an image of the radar backscatter of the terrain is acquired in polar coordinates. This image contains both road and off-road scatter components which must be segmented from each other. Geometric constraints on the road edges are naturally formulated in the Cartesian cartographic domain. However, to use the recorded data directly, we apply the road constraints in polar coordinates. Moreover, our estimator is based on a criterion which is largely insensitive to the off-road scatter. Numerical results are given for real data and illustrate the accuracy and robustness of our approach. Finally we derive the Fisher information matrix for evaluation of the achievable accuracy of segmentation for our model via the Cramèr Rao bound.

1 Introduction

The recovery of road edges from front-mounted radar and optical sensors has been of recent interest in intelligent highway vehicle systems (IVHS) and present several challenges. In particular edge detection must have high reliability and be robust to many changing conditions such as: weather, visibility, clutter and noise, road surface variability, presence of cross streets, exits, crosswalks, etc. To this end, we need a fairly simple model, a segmentation criterion which is easy to optimize, and fast convergence.

We propose such an algorithm, which is based on estimation of a pair of tightly coupled parabolic curves defined in the cartographic domain and which are transformed to the polar domain of the raw image acquisition. Our method performs curve estimation directly in the polar domain. Robustness to off-road clutter is achieved by using a non-linear least squares criterion which involves only estimated road pixels for which faithful priors are available. This

simplification allows a simple numerical optimization to be performed, without resorting to time consuming Monte Carlo methods. An issue which is currently under study is the choice of search space for the parameter optimization. We illustrate the proposed technique with real images acquired in Michigan from an L band radar mounted on a military transport vehicle on a country road.

As the segmented images will serve as a basis for collision avoidance, lane following and other critical decisions, assessing the accuracy of the segmentation is of paramount importance. To this end we derive lower bounds on minimum achievable mean square error of any segmentation method. This requires reformulation of the likelihood of the observation system in a continuous (non-pixelated) setting which permits the derivation of general expressions for the Fisher information matrix which generalize the results of the analysis [4] for edge detection.

2 The Main Assumptions

The segmentation procedure will be developed in this paper under the following assumptions.

- (a) A road has a regular profile which can be modeled using a smooth function. Moreover, the road width is constant inside the field of view.
- (b) Data z determine a field of view with azimuth between -31° and 32° and a range of up to 128 meters.
- (c) The road has constant curvature within the field of view. Given the fact that the field of view is restricted, this assumption is realistic.
- (d) The road is a truly homogeneous region. No assumption is given for the off-road zones.
- (e) The angular resolution of the radar data decreases linearly with distance.

3 Parabolic road edge model

A birds-eye view of the road, which we call the cartographic domain, is represented on a Cartesian lattice with axes (x, y) . The left and right edges of the road, \mathcal{X}_l and \mathcal{X}_r respectively, are defined as functions of the vertical axis y . Following [8, 2], these are modeled using parabolic curves:

$$\mathcal{X}_l(y) = ay^2 + by + c_l, \quad \mathcal{X}_r(y) = ay^2 + by + c_r \quad (1)$$

where a , b and c_l , c_r are the parameters that we shall seek. The subscript l and r will indicate “left” and “right”. Since the vehicle is inside the road, $c_r > 0$ and $c_l = c_r - d < 0$, where d is the width of the road. The recorded image z is acquired on a rectangular area (φ, ρ) whose axes, angular position $\varphi \in [-31\pi/180, 32\pi/180]$ and range $\rho \in [1/2, 128]$, are the transform in polar coordinates of the Cartesian coordinates, $x = \rho \sin \varphi$ and $y = \rho \cos \varphi$. However, the model for the road edges is naturally defined in the (x, y) domain. An issue is to transform data z into the (x, y) domain: such an approach has been used in [8] which has the advantage of simplifying calculations. The drawbacks are that interpolating data into the cartographic domain generates errors which can be amplified during the edge detection stage and makes it difficult to exploit the advantages of (e).

Similarly to [10, 5], we transform the cartographic edge model (1) into the polar domain. In polar coordinates, the road edges are denoted by \mathcal{R}_c for $c \in \{l, r\}$ and satisfy

$$\mathcal{R}_c \sin \varphi = a\mathcal{R}_c^2 \cos^2 \varphi + b\mathcal{R}_c \cos \varphi + c_c$$

Solving this equation with respect to (w.r.t.) \mathcal{R}_c yields:

- if $ac_{l,r} \leq 0$ (2)

$$\mathcal{R}_c(\varphi) = \frac{-\mathcal{B}(\varphi) + \text{sign } a \sqrt{\mathcal{B}^2(\varphi) + 4|ac_{l,r}| \cos^2 \varphi}}{2a \cos^2 \varphi}$$

$$\text{where } \mathcal{B}(\varphi) = b \cos \varphi - \sin \varphi$$

- if $ac_{l,r} > 0$ (3)

$$\mathcal{R}_c(\varphi) = \frac{-\mathcal{B}(\varphi) \pm \sqrt{\mathcal{B}^2(\varphi) - 4ac_{l,r} \cos^2 \varphi}}{2a \cos^2 \varphi}$$

$$\text{where } \begin{cases} \varphi \leq \arg \tan(-2\sqrt{ac_{l,r}} + b) & \text{if } a < 0 \\ \varphi \geq \arg \tan(2\sqrt{ac_{l,r}} + b) & \text{if } a > 0 \end{cases}$$

When $ac_{l,r} > 0$, each edge \mathcal{R}_c takes two different values for the same φ which correspond to the cases + and - in (3). Based on this, our scene is partitioned into left off-road \mathcal{T}_l , road \mathcal{T}_s and right off-road \mathcal{T}_r . In the following, the subscript s will be used to address the road.

4 Segmentation Method

Actual radar image z is given on a discrete lattice, $\{(\varphi_j, \rho_i), -M/2 + 1 \leq j \leq M/2, 1 \leq i \leq N\}$ (where we sup-

pose M is even). After discretization of \mathcal{R}_l and \mathcal{R}_r along the ρ -axis, (2) is inverted and the angular position of the road edges is expressed as a function of the range, $\Phi_l(\rho_i)$ and $\Phi_r(\rho_i)$ for $1 \leq i \leq N$. Road \mathcal{T}_s ,

$$\mathcal{T}_s(a, b, c_r, d) = \{(i, j) : \Phi_l(\rho_i) \leq j\pi/180 \leq \Phi_r(\rho_i)\}$$

is a function of the model parameters, so estimating its edges amounts to determine the optimal $\hat{a}, \hat{b}, \hat{c}_r, \hat{d}$.

The likelihood function of the radar image is given by a log-normal distribution [1, 6, 8]:

$$P(z|a, b, c_r, d) = \prod_{c \in \{s, l, r\}} \prod_{(i, j) \in \mathcal{T}_c} \frac{\exp\left[-\frac{(\log z_{i,j} - \mu_c)^2}{2\sigma_c^2}\right]}{z_{i,j} \sqrt{2\pi\sigma_c^2}} \quad (4)$$

where σ_c^2 is the variance of the region c . For convenience, we will use log-data $y_{i,j} := \log z_{i,j}$.

Many authors [6, 9, 5] conceived algorithms based on the maximization of (4). Let us emphasize that *the model in (4) supposes all three regions, \mathcal{T}_c , $c \in \{s, l, r\}$, are homogeneous*. Although the road is homogeneous, nothing is known about the side regions. So, we wish to build a method which is insensitive to the off-road scatter components. Our approach is based on several arguments which are exposed below.

(i) Criterion involving only the pixel of the road. Observe that if we are given the road width \hat{d} , a simple criterion, involving only the pixels of the road, is straightforward:

$$\begin{aligned} \mathcal{J}(a, b, c_r; \hat{d}, y) &= \frac{\sum_{(i,j) \in \mathcal{T}_s(\cdot)} (y_{i,j} - \hat{\mu}_s)^2}{\#\{\mathcal{T}_s(a, b, c_r, \hat{d})\}} \\ \hat{\mu}_s &= \frac{\sum_{(i,j) \in \mathcal{T}_s(a, b, c_r, \hat{d})} y_{i,j}}{\#\{\mathcal{T}_s(\cdot)\}} \end{aligned} \quad (5)$$

where # stands for cardinality and $\hat{\mu}_s$ is the empirical mean over the road. Parameters a, b, c_r are estimated as

$$(\hat{a}, \hat{b}, \hat{c}_r) = \arg \min_{a, b, c_r} \mathcal{J}(a, b, c_r; \hat{d}, y) \quad (6)$$

The proposed method (5-6) is to search over the recorded image for *the patch of constant width and curvature which has the minimum variance, i.e. which is the most homogeneous*. This is a sound objective which leaves the side regions \mathcal{T}_l and \mathcal{T}_r out of consideration, and thus improves robustness to off-road variability (d).

(ii) Estimation of the road width from a short-range section. From (e), the road width d is reliably represented only in data corresponding to a few tens of meters

in front of the vehicle. Over such a section, the road edges can be assumed linear. We propose to estimate d from a section of the road of length ℓ , denoted by z_ℓ , by maximizing (1) where we fix $a = 0$:

$$(\hat{b}', \hat{c}_r, \hat{d}) = \arg \min_{b, c_r, d} \mathcal{G}(b, c_r, d) \quad (7)$$

$$\text{where } \mathcal{G}(b, c_r, d) = -\log P(z_\ell | a = 0, b, c_r, d) \quad (8)$$

From (8), we will keep only \hat{d} . The road edges relevant to this linear model, say $\tilde{\mathcal{R}}_c$ for $c \in \{l, r\}$, read

$$\tilde{\mathcal{R}}_c(\varphi) = \frac{c_{l,r}}{\sin \varphi - b \cos \varphi}. \quad (9)$$

By inverting (9), the angular position of the road edges is:

$$\tilde{\Phi}_{l,r}(\rho) = 2 \arctan \frac{-\rho + \sqrt{(1+b^2)\rho^2 - c_{l,r}^2}}{b\rho - c_{l,r}}. \quad (10)$$

Having a simple, explicit expression for the edges of the road is an important factor to speed up the calculations relevant to this stage.

A finer tuning of \hat{d} can be obtained by allowing $a \neq 0$ in (7) and performing a local minimization of \mathcal{G} in the vicinity of the already obtained estimate of the width of the road.

(iii) Numerical simplifications allowing “exhaustive” minimization. In spite of their quadratic form, both criteria \mathcal{J} and \mathcal{G} are multimodal w.r.t. the parameters we seek. In a similar context, EM minimization has been proposed in [7] and Metropolis optimization in [9, 5]. Being based directly on (4), such methods typically involve all the pixels of z .

In contrast, the approach proposed in (i) and (ii) allows calculations over reduced regions, since both criteria \mathcal{J} and \mathcal{G} concern only a small parcel of the image. The linear assumption in (ii) greatly simplifies the calculations as well. In addition, our edge model depends on a very restricted number of parameters. All these facts permit an optimization by “exhaustive” search to be envisaged. Global minimization of \mathcal{J} and \mathcal{G} is performed using a constrained “exhaustive” search over a discrete grid of sampled values of the parameters. The numerical efficiency of such a method critically depends on the number and the distribution of parameter samples which are used for the “exhaustive” search. Next, we suggest how to reduce the number of samples by restricting the search domain.

(iv) Region of interest for the parameters.

• *A priori known feasibility domain:* this domain contains all the parameters yielding a pair of road edges which remains in the field of view for at least \mathcal{L} meters:

$$|av^2 + bv| \leq vF \quad \text{for } 0 \leq v \leq \mathcal{L} \quad (11)$$

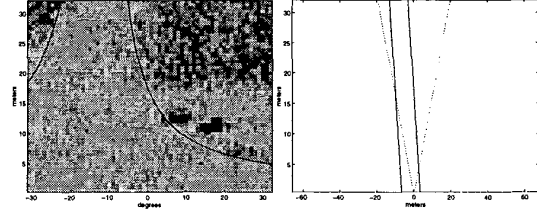


Figure 1: Coarse estimate of road width from the front parcel of the road, using a linear model for the road edges.

where $F = \frac{1}{2}(\tan \frac{32\pi}{180} + \tan \frac{-31\pi}{180})$. Note that $-vF$ and vF are the boundaries of the field of view.

The order of magnitude for c_r comes from the fact that c_r is the distance between the car and the right edge of the road. The width of the road d is larger than the width of a car.

• *Coarse segmentation of the road.* Next, we use a simple coarse estimation procedure to obtain a reduced region of interest (ROI) which contains the road with high probability. The idea is the following. The image is partitioned into several sections and in each of them the road edges are modeled by linear segments, similarly to (9-10). More precisely, a term of the form (5) is defined over each segment, starting from the second segment, since the first one has been estimated by (7) in the context of (ii). Let us stress that each road segment is described using only one parameter b , since $a = 0$ and c_r are fixed by the constraint that road is continuous.

Although the so obtained road estimate exhibits sharp corners, it provides a faithful approximation of its shape. Stress that such a locally linear model is not very sensitive to the fineness of the sampling of the parameters. This coarse estimate is very rapid to compute.

5 Experimental results

In this section road segmentations are shown in the domain of the data, *i.e.* in the polar domain (φ, ρ) . Next to these segmentations is plotted the corresponding birds-eye view of the road in the (x, y) -domain, and the radar sensor field of view is plotted with a dotted line and has a V-shaped boundary.

Fig. 1 shows a coarse estimate of road width using the linear model for the road edges, as given in (7-8). For $\ell = 30\text{m}$, this yields an estimate $\hat{d} = 10\text{m}$.

A refined parabolic estimate of road width is obtained by finding the least squares fit for arbitrary $a \neq 0$ in (8). The result is given in Fig. 2 confirming that $\hat{d} = 10\text{m}$.

The segmentation presented in Fig. 3 corresponds to $\hat{a} =$

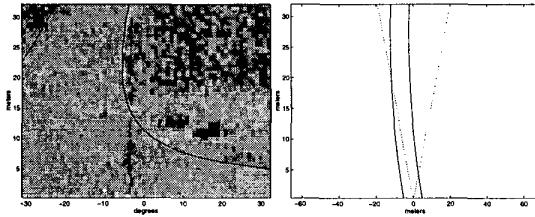


Figure 2: Refined estimate of road width from the same parcel of the road using a parabolic model for the road edges.

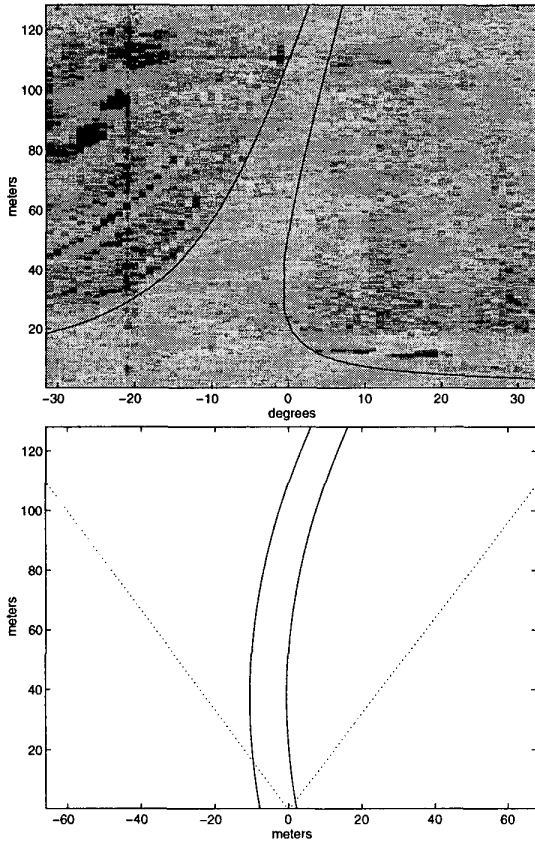


Figure 3: The final segmentation obtained using the proposed algorithm faithfully retrieves the locations of the road edges.

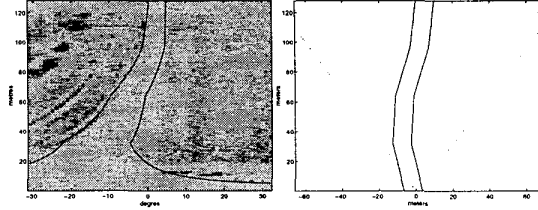


Figure 4: Coarse and rapid segmentation of the road using a locally linear model for its edges. It provides a faithful ROI for a further estimation of the location of the road.

0.002, $\hat{b} = 0.1476$ and $\hat{c}_r = 2.25$ and has been calculated using (5-6). The edges of the road are correctly retrieved and it is seen that the road has a gentle right turn.

The global minimization of criteria \mathcal{J} and \mathcal{G} has been performed using a constrained “exhaustive” search over a discrete grid of sampled values of the parameters. First we sample only over the *a priori* known feasibility domain. Second, we used a coarse estimation with 4 sections. It can be seen from Fig. 4 that our ROI surrounds the above estimate: more closely just in front of the car and more loosely with the increase of the distance from the car. This ROI yields an additional set of strong but meaningful constraints for the parameters of the parabolic model.

6 Continuous-array Log-likelihood

The method proposed in this paper yields a pertinent segmentation of the road edges. However, it is critical to know whether such results can be obtained in a broad range of situations. Closely related questions are (i) what is the best sampling for the radar data, (ii) what should be the extent of the section of the road ℓ allowing to get a faithful estimate of the road width, (iii) is it pertinent to undersample some areas in the image, (iv) what is the best sampling for the parameters modeling the road. Rigorous indications for such questions are provided by the Fisher information matrix (FIM) of the parameters involved in both, data acquisition and subsequent segmentation. Our next ambition is then to determine the FIM corresponding to the main parameters involved in our model.

FIM is naturally formulated over continuous-grid images. Put $\xi = (\phi, \rho)$ where ϕ and ρ are reals. By assumption (b) and (1), the ideal road scene f is composed of three constant patches of constant level μ_c

$$f(\xi) = \mu_l \mathbb{I}_l(\xi) + \mu_s \mathbb{I}_s(\xi) + \mu_r \mathbb{I}_r(\xi) \quad (12)$$

where $\mathbb{I}_c(\xi) := \mathbb{I}(\xi \in \mathcal{T}_c)$ is the characteristic function of the c th region ($\mathbb{I}(S) = 1$ when S is true and $\mathbb{I}(S) = 0$ otherwise). Here the continuous image model is developed using log-data $y(\xi) = \log z(\xi)$ Gaussian radar measurement

model. This data set is a modification of (12), degraded by Gaussian perturbations. The measurement is assumed to consist of three additive components: noise $w(\xi)$ which is spatially white, zero-mean and Gaussian with stationary variance η ; a specific terrain-dependent clutter $n_c(\xi)$ which characterizes each terrain type (road and offroad) \mathcal{T}_c . It is supposed Gaussian with mean zero, whereas its covariance $\mathcal{K}_c(\xi, \xi')$ is non-white. It is convenient to assume that \mathcal{K}_c is zero beyond the support of the c th region, *i.e.* $\mathcal{K}_c(\xi, \xi') = \mathcal{K}_c(\xi, \xi') \mathbb{I}_c(\xi) \mathbb{I}_c(\xi')$ for every c . The reflection noise on the entire scene can be expressed as $\sum_{c \in \{s, l, r\}} n_c(\xi) \mathbb{I}_c(\xi)$.

Being bandlimited, the observation system introduces spatial smoothing over both the image f and the noise process n . We model this phenomenon as

$$\Phi_h(\xi) = \frac{1}{2\pi h} \exp\left(-\frac{\|\xi\|^2}{2h}\right)$$

where h is related to the amount of blur. This yields a “mean image” and a “blurred noise” process

$$\begin{aligned} m(\xi) &= (\Phi_h * f)(\xi) \\ n(\xi) &= \sum_{c \in \{s, l, r\}} (\Phi_h * n_c \mathbb{I}_c)(\xi) \end{aligned}$$

The log-data $y(\xi)$ finally reads

$$y(\xi) = m(\xi) + n(\xi) + w(\xi)$$

All noise-processes being zero-mean, we get $E[y(\xi)] = m(\mathbf{v})$. The covariance of y , say $\mathcal{K}(\xi, \xi')$, reads

$$\begin{aligned} \mathcal{K}(\xi, \xi') &= \delta(\xi - \xi') + \mathcal{K}_w(\xi, \xi') \\ \text{where } \mathcal{K}_w(\xi, \xi') &= \Phi_h * \left(\sum_c \mathcal{K}_c\right) * \Phi_h \end{aligned}$$

Above, \mathcal{K}_w is the covariance of the blurred clutter.

In the following, θ will denote a vector which contains all the parameters involved in our model. Some of these parameters are geometrical: a, b, c_r and d . The remaining are related to the statistical model: μ_c, σ_c for $c \in \{l, s, r\}$, and h , in addition to the parameters involved in all \mathcal{K} 's. So we can write down $\mathcal{K}(\xi, \xi'; \theta)$ and $\mathcal{K}_w(\xi, \xi'; \theta)$, *etc.*

The likelihood function of y is derived using a Karhunen-Loeve decomposition of \mathcal{K} . Let $\lambda_i(\theta)$ and $\psi_i(\cdot; \theta)$ be the eigenvalues and the eigenfunctions, respectively, of $\mathcal{K}_w(\xi, \xi'; \theta)$. Define

$$\begin{aligned} m_i(\theta) &= \int m(\xi; \theta) \psi_i(\xi; \theta) d\xi \\ y_i &= \int y(\xi) \psi_i(\xi; \theta) d\xi \end{aligned}$$

It can be shown that y_i are Gaussian variables with mean $m_i(\theta)$ and covariance

$$E\{[y_i - m_i(\theta)][y_j - m_j(\theta)]\} = [1 + \lambda_i(\theta)] \mathbb{I}(i = j)$$

Following [11], we calculate the likelihood function relevant to y_i for $i = 1, \dots, k$. Letting $k \mapsto \infty$ finally yields

$$\ln \Lambda(y; \theta) = - \sum_{i=1}^{\infty} \frac{\ln[1 + \lambda_i(\theta)]}{2} - \sum_{i=1}^{\infty} \frac{[y_i - m_i(\theta)]^2}{2[1 + \lambda_i(\theta)]} + \sum_{i=1}^{\infty} y_i^2$$

An equivalent space-domain representation of $\ln \Lambda$ comes from the observation that the second term in the above expression can be put into the form:

$$\begin{aligned} \sum_{i=1}^{\infty} \frac{[y_i - m_i(\theta)]^2}{1 + \lambda_i(\theta)} &= \int \int d\xi d\xi' \times \\ &[y(\xi) - m(\xi; \theta)][y(\xi') - m(\xi'; \theta)] \mathcal{K}^{-1}(\xi, \xi'; \theta) \end{aligned}$$

The details of these derivations can be found in [3].

7 Fisher Information Matrix

Let θ_k and θ_l be two parameters among the entries of θ . The FIM has entries F_{kl} which are given by partial derivatives of the log likelihood function [11]

$$F_{kl} = E \left[\frac{\partial \ln \Lambda(y; \theta)}{\partial \theta_k} \frac{\partial \ln \Lambda(y; \theta)}{\partial \theta_l} \right]$$

F_{kl} can equivalently be expressed *via* the second derivative of $\ln \Lambda$ w.r.t. (θ_k, θ_l) . It offers some analytical facilities but supposes $\ln \Lambda$ twice differentiable, so we prefer to not to use it. After some developments, detailed in [3], we get

$$\begin{aligned} F_{kl} &= \frac{1}{2} \sum_{i=1}^{\infty} \frac{1}{[1 + \lambda_i(\theta)]^2} \frac{\partial \lambda_i(\theta)}{\partial \theta_l} \frac{\partial \lambda_i(\theta)}{\partial \theta_k} \\ &+ \sum_{i=1}^{\infty} \frac{1}{1 + \lambda_i(\theta)} \frac{\partial m_i(\theta)}{\partial \theta_k} \frac{\partial m_i(\theta)}{\partial \theta_l} \end{aligned}$$

An equivalent space domain form of F_{kl} is derived by remarking that series relevant to $[1 + \lambda_i(\theta)]^{-1}$ are related the inverse of the clutter covariance \mathcal{K} :

$$\begin{aligned} F_{kl} &= \frac{1}{2} \int du \int d\xi' \int d\xi \mathcal{K}^{-1}(\xi, u; \theta) \frac{\partial \mathcal{K}(\xi, \xi'; \theta)}{\partial \theta_k} \\ &\times \int dv \mathcal{K}^{-1}(\xi', v; \theta) \frac{\partial \mathcal{K}(v, u; \theta)}{\partial \theta_l} \\ &+ \int d\xi \int d\xi' \mathcal{K}^{-1}(\xi, \xi'; \theta) \frac{\partial m(\xi; \theta)}{\partial \theta_k} \frac{\partial m(\xi'; \theta)}{\partial \theta_l} \end{aligned}$$

All entries $F_{k,l}$, for which θ_k is a geometrical parameter whereas θ_l is a statistical parameter, are null. This fact confers a block-diagonal structure on F .

Geometrical information

These are the terms of F for which both θ_k and θ_l are elements of $\{a, b, c_l, d\}$. Such parameters are involved in F_{kl}

only through the shape of the \mathbb{I}_c 's. In order to make this relation explicit, we express \mathcal{K}_u as

$$\mathcal{K}_u(\xi, \xi'; \theta) = \sum_c \int_{\mathcal{T}_c} \int_{\mathcal{T}_c} dudv \Phi_h(\xi - u) \Phi_h(\xi' - v) \mathcal{K}_c(u, v; \theta)$$

Then we find

$$\frac{\partial \mathcal{K}(\xi, \xi'; \theta)}{\partial \theta_k} = 2 \sum_c \int du \int dv \Phi_h(\xi - u) \Phi_h(\xi' - v) \mathcal{K}_c(u, v; \theta) \frac{\partial \mathbb{I}_c(v)}{\partial \theta_k}$$

where we use the symmetry of \mathcal{K}_c . In the above expression, $\frac{\partial \mathbb{I}_c(v)}{\partial \theta_k}$ consists of Dirac distributions placed along the boundary of \mathcal{T}_c . This provides a closed-form way to differentiate the boundaries of the integration areas which is equivalent to the Leibnitz rule, see [3]. This part of the FIM provides a bound on accuracy of the segmentation.

Statistical information

Next we focus on the terms of F relevant to the statistical parameters. In order to simplify the analysis, assume that

$$\mathcal{K}(\xi, \xi'; \theta) = \alpha_c \exp\left(-\frac{\|\xi - \xi'\|^2}{2\beta_c}\right)$$

Then the model of the covariance of the data is:

$$\mathcal{K}(\xi, \xi', \theta) = \delta(\xi - \xi') + \sum_c \int_{\mathcal{T}_c} \int_{\mathcal{T}_c} dudv \frac{\alpha_c G(\xi, \xi', u, v; h, \beta_c)}{4\pi^2 h^2}$$

$$G(\xi, \xi', u, v; h, \beta_c) := \exp\left(-\frac{\|\xi - u\|^2 + \|\xi' - v\|^2}{2h} - \frac{\|u - v\|^2}{2\beta_c}\right)$$

The parameters of interest are h as well as μ_c, α_c and β_c for $c \in \{l, s, r\}$. The derivatives of \mathcal{K} , involved in the expression of $F_{k,l}$ are straightforward.

- Derivatives w.r.t. the parameters involved in \mathcal{K} :

$$\frac{\partial \mathcal{K}(\xi, \xi', P)}{\partial \alpha_c} = \int_{\mathcal{T}_c} \int_{\mathcal{T}_c} dudv \frac{G(\xi, \xi', u, v; h, \beta_c)}{4\pi^2 h^2}$$

$$\frac{\partial \mathcal{K}(\xi, \xi', P)}{\partial \beta_c} = \int_{\mathcal{T}_c} \int_{\mathcal{T}_c} dudv \frac{\alpha_c \|u - v\|^2 G(\xi, \xi', u, v; h, \beta_c)}{8\pi^2 h^2 \beta_c^2}$$

- Derivative w.r.t. h :

$$\frac{\partial \mathcal{K}(\xi, \xi', P)}{\partial h} = \sum_c \int_{\mathcal{T}_c} \int_{\mathcal{T}_c} dudv \frac{\alpha_c G(\xi, \xi', u, v; h, \beta_c)}{8\pi^2 h^4} (\|\xi - u\|^2 + \|\xi' - v\|^2 - 4h)$$

- Derivatives of the mean image m :

$$\frac{\partial m(\xi; \theta)}{\partial h} = \sum_c \frac{\mu_c}{4\pi h^3} \int_{\mathcal{T}_c} d\xi' (\|z\|^2 - 2h) \exp\left(-\frac{\|z\|^2}{2h}\right)$$

$$\frac{\partial m(\xi; \theta)}{\partial \mu_c} = \int_{\mathcal{T}_c} d\xi' \Phi_h(\xi - \xi')$$

The last step will be to evaluate numerically the FIM for typical road configurations. These will be presented in subsequent papers.

8 Concluding Remarks

We have presented a novel technique for estimating road edges from polar scan images acquired from vehicle-mounted radar sensors. The technique proposed is accurate, robust and simple to implement. Some issues which remain to be studied are the following. Iterative methods may be useful for reducing the computation time. Next, we provide theoretical expressions for the Fisher information of the parameters, involved in our segmentation. These will permit an objective measure of the performance of the segmentation, to be obtained.

References

- [1] J. Aitchison and J. Brown, *The Log-normal Distribution*, 1957, Cambridge University Press.
- [2] Y. Amit, U. Grenander and M. Piccioni, "Structural Image Restoration Through Deformable Templates", in *J. Am. Statist. Assoc.*, 1991, vol. 86, pp. 376-387.
- [3] A. Hero and M. Nikolova, "Fisher Information Matrix for segmented images", tech. report.
- [4] R. Kakarala and A. O. Hero, "On achievable accuracy in edge localization", in *IEEE Trans. on Pattern Recognition and Machine Intelligence (PAMI)*, Vol. 14, No. 7, pp. 777-781, July 1992.
- [5] K. Kaliyaperumal and S. Lakshmanan, "An Algorithm for Detecting Roads and Obstacles in Radar Images", to appear in *IEEE Trans on Vehicular Technology*.
- [6] S. Lakshmanan and D. Grimmer, "A Deformable Template Approach to Detecting Straight Edges in Radar Images", in *IEEE Trans. Pattern Anal. Mach. Intell.*, 1991, vol. 18, pp. 438-443.
- [7] J. Leite and E. Hancock, "Iterative curve organization with the EM algorithm", in *Pattern Recognition Letters*, 1997, vol. 18, n. 2, pp. 143-155
- [8] B. Ma, S. Lakshmanan and A. Hero, "Detection of Curved Road Edges in Radar Images Via Deformable Templates", in *Proceedings of IEEE ICIP*, 1997.
- [9] B. Ma, S. Lakshmanan and A. Hero, "Simultaneous Detection of Lane and Pavement Boundaries Using Model-Based Multisensor Fusion", submitted to *IEEE Transactions on Intelligent Transportation Systems (ITS)*.
- [10] M. Nikolova and A. Hero, "Segmentation of road edges from a vehicle-mounted imaging radar", *Proceedings of the IEEE Statistical Signal and Array Processing*, 1998, pp. 212-215.
- [11] H. Van Trees, "Detection, estimation and modulation theory", Part 3, Wiley, New York, 1968.